

# Harvest of functional mesenchymal stem cells derived from *in vivo* osteo-organoids

Shunshu Deng<sup>1,2,3</sup>, Fuwei Zhu<sup>1,2,3</sup>, Kai Dai<sup>1,2,3,4,\*</sup>, Jing Wang<sup>1,3,4,\*</sup>, Changsheng Liu<sup>2,3,4,5,\*</sup>

## Key Words:

anti-replicative senescence; *in vivo* osteo-organoid; mesenchymal stem cell; recombinant human bone morphogenetic protein 2; stem cell therapy

## From the Contents

<b>Introduction</b>	<b>270</b>
<b>Methods</b>	<b>271</b>
<b>Results</b>	<b>273</b>
<b>Discussion</b>	<b>276</b>

## ABSTRACT

Bone marrow-derived mesenchymal stem cells (BM-MSCs) play a crucial role in stem cell therapy and are extensively used in regenerative medicine research. However, current methods for harvesting BM-MSCs present challenges, including a low yield of primary cells, long time of *in vitro* expansion, and diminished differentiation capability after passaging. Meanwhile mesenchymal stem cells (MSCs) recovered from cell banks also face issues like toxic effects of cryopreservation media. In this study, we provide a detailed protocol for the isolation and evaluation of MSCs derived from *in vivo* osteo-organoids, presenting an alternative to autologous MSCs. We used recombinant human bone morphogenetic protein 2-loaded gelatin sponge scaffolds to construct *in vivo* osteo-organoids, which were stable sources of MSCs with large quantity, high purity, and strong stemness. Compared with protocols using bone marrow, our protocol can obtain large numbers of high-purity MSCs in a shorter time (6 days vs. 12 days for obtaining passage 1 MSCs) while maintaining higher stemness. Notably, we found that the *in vivo* osteo-organoid-derived MSCs exhibited stronger anti-replicative senescence capacity during passage and amplification, compared to BM-MSCs. The use of osteo-organoid-derived MSCs addresses the conflict between the limitations of autologous cells and the risks associated with allogeneic sources in stem cell transplantation. Consequently, our protocol emerges as a superior alternative for both stem cell research and tissue engineering.

<http://doi.org/10.12336/biomatertransl.2023.04.006>

**How to cite this article:**  
Deng, S.; Zhu, F.; Dai, K.; Wang, J.; Liu, C.  
Harvest of functional mesenchymal stem cells derived from *in vivo* osteo-organoids. *Biomater Transl.* 2023, 4(4), 270-279.



## Introduction

Mesenchymal stem cells (MSCs) are kinds of stem cells that widely exist in various tissues and organs of the adult body.<sup>1-3</sup> They have the potential for multi-lineage differentiation, such as osteogenic, adipogenic, myogenetic, chondrogenic, and neurogenic differentiation.<sup>2,4,5</sup> This makes MSCs a popular choice for research on cancer, ageing-related topics,<sup>6,7</sup> and stem cell engineering.<sup>8,9</sup> Because the MSCs still display strong proliferation and differentiation performance *in vitro*,<sup>1,10</sup> coupled with cytokine secretion and immune function,<sup>11-14</sup> they are often used in tissue engineering. This includes, but not limited to, research on coronavirus disease 2019 (COVID-19),<sup>15</sup> spinal cord injury,<sup>16</sup> femoral

head necrosis,<sup>17</sup> systemic lupus erythematosus,<sup>18</sup> and colitis.<sup>19</sup> Research models related to MSCs primarily use bone marrow,<sup>20</sup> compact bone,<sup>1,21</sup> peripheral blood,<sup>22</sup> adipose tissue,<sup>23</sup> urine<sup>24,25</sup> and joint synovium.<sup>3</sup> MSCs from various sources exhibit different characteristics because they tend to be different subtypes of stem cells. For adult humans, compared with other methods, isolation from bone marrow is a more established method for autologous stem cell extraction.<sup>26,27</sup> Bone marrow-derived MSCs (BM-MSCs) possess superior three-lineage differentiation capability compared with other adult tissue-derived MSCs. However, their lower yield, lower purity, and longer expansion cycle than allogeneic MSCs limit the clinical applications.

## Rapid obtaining strategy of massive MSCs

Recently, the concept of *in vivo* tissue engineering<sup>5, 14, 23</sup> co-constructed by cells and materials<sup>28, 29</sup> has emerged as a feasible solution for obtaining autologous stem cells. In previous work, we found that the gelatin sponge loaded with recombinant human bone morphogenetic protein 2 (rhBMP-2) formed periosteum-like tissues<sup>30</sup> rich in functional stem cells after being implanted in mice for several days. The periosteum-like tissue gradually developed into mature osteo-organoids with a bone marrow-like structure.<sup>31</sup> In previous experiments, we isolated stem cells from these osteo-organoids,<sup>32</sup> thus defining these cells as osteo-organoid-derived MSCs (odMSCs). Interestingly, based on the implantation site<sup>33</sup> and the cell phenotype,<sup>34</sup> it was speculated that these cells are related to myoideum, making osteo-organoids a stable source of this new subtype of BM-MSCs.

In this study, to better emphasise the advantages of odMSCs, we constructed osteo-organoids in the mouse hindlimb muscles, using the femur and tibia as controls. After isolation and culture, the MSCs were further evaluated, including the colony forming unit-fibroblast (CFU-F) experiment conducted before the primary cells were washed. The purified MSCs at passage 2 (P2) were used for flow cytometry, tri-lineage differentiation and proliferation assays. The odMSCs could be obtained in sufficient quantities in half the time compared with BM-MSCs. Besides, odMSCs showed better stemness and activity, even after multiple passages. Given the aforementioned advantages, we can conclude that this protocol for obtaining MSCs holds significant research value and broad application prospects.

## Methods

### Animals

We selected the C57BL/6J mouse strain (8 weeks, male, with an average weight of approximately 25 g) for our protocol. All mice were purchased from and housed in Shanghai Shengchang Biotechnology Co., Ltd. (Shanghai, China; license No. SCXK (Hu) 2021-0002) and housed at 22–23°C on a 12-hour light/dark cycle with free access to water and food, as indicated. All experimental procedures were approved by the Animal Care and Use Committee of the East China University of Science and Technology (approval No. ECUST-2022-053) on March 9, 2022. All efforts were made to minimise animal suffering.

### Preparation and implantation of rhBMP-2 loaded gelatin scaffolds

For implant preparation, 10 µL of rhBMP-2 (1 mg/mL in phosphate-buffered saline; Rebone Biomaterials Co., Shanghai, China) was absorbed by a gelatin scaffold (5 mm × 5 mm × 5 mm; Xiang'en Medical Technology Development Co., Nanchang, Jiangxi, China). The procedure was conducted under sterile conditions, then the scaffold was frozen at –20°C

for 4 hours and lyophilised for 8 hours. The rhBMP-2-loaded gelatin scaffolds were stored at –20°C.

To mitigate the potential interference of location differences *in vivo*, the source of MSCs was selected in hindlimbs. For osteo-organoid generation, mice were anaesthetised (ZS-MV-IV; Hetian Scientific Instruments Co., Shanghai, China; isoflurane, 0.5% of the maximal flow, inhalation). Subsequently, two scaffolds were implanted in the muscle of both hindlimbs, respectively. Once revived on a warming station, the mice were allowed to eat and drink *ad libitum* as usual.

### Isolation of MSCs from osteo-organoids

A buffer for cell suspension was prepared using 2% fetal bovine serum (Gibco, Grand Island, NY, USA) in Hank's balanced salt solution (with Ca<sup>2+</sup>/Mg<sup>2+</sup>; Gibco). After 5 days of feeding, the mice were anaesthetised with isoflurane inhalation, and then terminated by cervical dislocation. They were placed in a beaker where the whole body was immersed in 75% (v/v) ethanol for 3 minutes, and then the body was transferred to biosafety cabinet. To prevent contamination of the countertop, sterile gauze was placed in advance (**Figure 1A**). Skin and muscle between hindlimbs and trunk were removed by ophthalmic scissors with little or no bleeding. Subsequently, the feet and the entire skin on the hindlimbs were removed. After that, the trochanter major was cut off (**Figure 1B**) allowing for the entire leg. Typically, the osteo-organoids could be found in the hamstrings (**Figure 1C**). Once isolated from the muscle, the osteo-organoids were immersed in a 60-mm cell culture dish (Corning Incorporated, Corning, NY, USA) containing 3 mL of the cell suspension buffer (**Figure 1D**). Osteo-organoids were first cut and then shredded in different shear directions by curved blade ophthalmic scissors (**Figure 1E and F**). Finally, all osteo-organoid fragments, including the buffer, were transferred to a sterile 15-mL Falcon tube. In addition, native bone marrows from femora and tibia were flushed out by syringe as a traditional method.<sup>20</sup>

The tubes containing bone marrow or osteo-organoid fragments were centrifuged at 300 × g for 10 minutes to remove the supernatant. Meanwhile the digestive enzyme mixture was prepared. Each 1 mL of this mixture contained: stock of collagenase type I (Worthington, Lakewood, NJ, USA) 100 µL, neutral protease (Roche, Basel, Switzerland) 100 µL and DNase (Mkbio, Shanghai, China) 20 µL in 800 µL Hanks' balanced salt solution (containing Ca<sup>2+</sup>/Mg<sup>2+</sup>).<sup>35</sup> This mixture was then added to the tubes containing the tissue pellets from bone marrow or osteo-organoid fragments. Then the tissue pellets were kept static for digestion at 37°C for 15 minutes. The tissue pellets were then left undisturbed for digestion at 37°C for 15 minutes. The tissue pellets were

1 State Key Laboratory of Bioreactor Engineering, East China University of Science and Technology, Shanghai, China; 2 Key Laboratory for Ultrafine Materials of the Ministry of Education, East China University of Science and Technology, Shanghai, China; 3 Engineering Research Center for Biomedical Materials of the Ministry of Education, East China University of Science and Technology, Shanghai, China; 4 Frontiers Science Center for Materiobiology and Dynamic Chemistry, East China University of Science and Technology, Shanghai, China; 5 Shanghai University, Shanghai, China

### \*Corresponding authors:

Kai Dai, daikai233@foxmail.com; Jing Wang, biomatwj@163.com; Changsheng Liu, liucs@ecust.edu.cn.

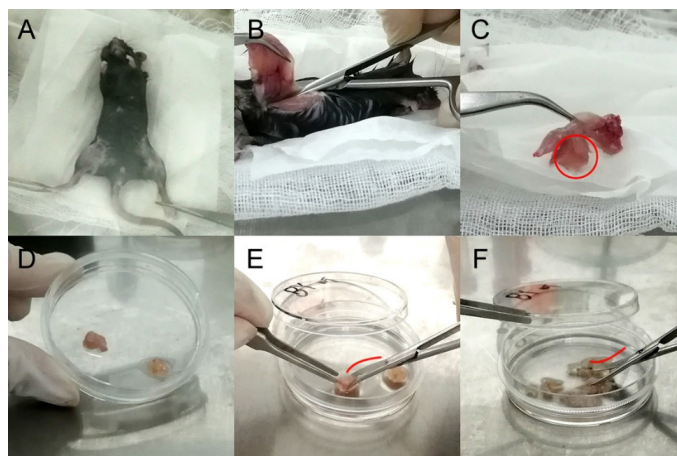


**Figure 1.** Illustrations of osteo-organoid cell separation procedures. (A) The mouse body soaked in 75% (v/v) ethanol was placed in biosafety cabinet. (B) After removing skin and muscle, a hindlimb was completely cut off, so that the femur and tibia could be used for extraction of bone marrow-derived mesenchymal stem cells (BM-MSCs). (C) The osteo-organoid was hidden in the swollen part of the muscle (red circle) between femur and calf. (D) Osteo-organoids covered with periosteum-like tissue were separated in a 60-mm cell culture dish. (E) The surface of the blade was convex (red curve) to cut the osteo-organoids. (F) The surface of the blade was concave (red curve) to shred the osteo-organoids.

resuspended using a vortex mixer and subsequently deposited on ice for 1 minute. The cell suspension extracted by digestion was then added to 10 mL of digestive enzyme neutraliser (0.4% ethylenediaminetetraacetic acid (0.5 M; Gibco) and 2% fetal bovine serum in Hanks' balanced salt solution (containing  $\text{Ca}^{2+}/\text{Mg}^{2+}$ )), followed by centrifugation at  $300 \times g$  for 10 minutes to remove the supernatant. To yield more cells, the digested tissue pellets could undergo another round of digestion and the subsequent operations were repeated.

#### Culture and purification of MSCs from osteo-organoids

The collected cells were resuspended in 1 mL of the cell

suspension buffer using trimmed pipette tips to minimise cell damage. The cell suspension was then filtered through a 70- $\mu\text{m}$  filter mesh to remove any fragments or cell clumps. When the complete medium (minimal essential medium  $\alpha$  (nucleosides; Gibco) supplemented with 20% fetal bovine serum, 1% penicillin-streptomycin (10,000 U/mL; Gibco), 1% sodium pyruvate (100 mM; Gibco) and 0.1% Rho-associated kinase inhibitor (Y-27632 dihydrochloride; 1 mL in dimethyl sulfoxide (10 mM); MedChemExpress, Monmouth Junction, NJ, USA)) had been warmed up in cell incubator, the cell suspension was seeded in 6-well plates or 100-mm cell culture dish (**Table 1**) containing the medium.

**Table 1.** Details of cell culture in different experiments

Experiment	Culture vessel	Volume of medium	Seeding density	Other suggestions
Colony forming unit-fibroblast	6-well plate	2 mL per well	$5 \times 10^5$ cells per well	Replace $\alpha$ -MEM with DMEM to prepare the complete medium
Purification	100-mm dish	15 mL per dish	$1 \times 10^7$ cells per dish	Culture under the condition of 5% $\text{O}_2$ atmosphere
Differentiation	6-well plate	2 mL per well	$2 \times 10^5$ cells per well	Use $\alpha$ -MEM containing 10% fetal bovine serum and 1% penicillin-streptomycin as the medium before differentiation assays
Proliferation	60-mm dish	5 mL per dish	$2 \times 10^5$ cells per well	Incubate the MSC for 2 hours in a medium containing 50 $\mu\text{M}$ EdU

Note: DMEM: Dulbecco's modified Eagle medium; EdU: 5-ethynyl-2'-deoxyuridine; MSC: mesenchymal stem cell;  $\alpha$ -MEM: minimal essential medium  $\alpha$ .

Once evenly dispersed, the cells were cultured in a cell incubator at  $37^\circ\text{C}$  under normal oxygen conditions. The culture medium was refreshed the following morning and every 3 days thereafter. Adherent cells were washed with Dulbecco's phosphate-buffered saline before adding fresh medium, thus purifying the MSCs. The primary cells were referred to passage 0 (P0) cells.

When MSCs reached 70–90% confluence, they could be passaged. That is, cells were washed twice with Dulbecco's

phosphate-buffered saline and then digested using 600  $\mu\text{L}$  (per 100-mm dish) of 0.25% trypsin (with phenol red; Gibco) at  $37^\circ\text{C}$ , for no longer than 2 minutes. This medium was used to wash the cells until the MSCs were completely detached from the bottom of the dish. The medium was used to wash cells until the MSCs were completely detached from the bottom of the dish. For passaging at a split ratio of 1:3, 2 mL of the cell suspension per dish was transferred to a new dish with the complete medium. The above procedures were based on the characteristics of MSCs (**Table 2**).

**Table 2. Purification operations are based on the characteristics of MSCs**

Characteristics	Operations
Adhesion of MSCs are earlier than other cells from marrow	Wash cells using Dulbecco's phosphate-buffered saline after seeding overnight
MSCs are easy to be digested and suspended	Time of digestion during the cell passage is not recommended to exceed 2 minutes
Low oxygen pressure increases the proliferation and reduces spontaneous differentiation of MSCs	Expand cells under the hypoxic condition (5% O <sub>2</sub> )

Note: MSCs: mesenchymal stem cells.

### ***In vitro* multilineage differentiation and cell proliferation assays**

MSCs were cultured in 6-well plates (or in a 15-mL Falcon tube for chondrogenic differentiation) in preparation for differentiation and proliferation experiments (Table 1). The operations of osteogenic, adipogenic, and chondrogenic differentiation were respectively performed according to the manual of OriCell™ Mesenchymal Stem Cell Osteogenic/Adipogenic/Chondrogenic Differentiation Medium (Cyagen Biosciences, Santa Clara, CA, USA). Cell proliferation was measured by 5-ethynyl-2'-deoxyuridine (EdU) assay, and the operations were performed according to the manual of BeyoClick™ EdU Cell Proliferation Kit (Beyotime, Shanghai, China).

### **CFU-F assay and flow cytometry**

For CFU-F assay, MSCs extracted from osteo-organoids were directly cultured in 6-well plates for 5 days (Table 1). After washed using Dulbecco's phosphate-buffered saline, the MSCs were fixed using 4% (w/v) paraformaldehyde for 30 minutes and then stained using toluidine blue (0.1%; Yuanye Biotechnology Co., Shanghai, China). After being washed using ddH<sub>2</sub>O, the colony formation could be observed under an optical microscope (DMI8; Leica, Hessan, Wetzlar, Germany).

For flow cytometry, purified MSCs were cultured until they reached 80–90% confluence. After washed using Dulbecco's phosphate-buffered saline and digested, MSCs they were stained using fluorescent antibodies in flow tubes and then analysed by flow cytometry. The cell aliquots were incubated: fluorescein isothiocyanate-conjugated CD45 or phycoerythrin-conjugated CD44, CD29 and CD31 or Alexa Fluor 700-conjugated stem cell antigen-1 and CD11b or Allophycocyanin-conjugated CD105 and CD140a (BD Biosciences, San Jose, CA, USA). The incubation was carried out at 4°C for 30 minutes in the dark. The cells were resuspended in 300 µL cell staining buffer (BD Biosciences) after washing. The flow cytometric analysis, including the test of EdU assay cell proliferation, was operated on CytoFLEX LX flow cytometer (Beckman Coulter, Brea, CA, USA). The data were analysed using FlowJo X (Three Star, San Carlos, CA, USA).

### **β-Galactosidase assay**

MSCs were cultured in 6-well plates before cells reached 100% confluence, with other culture conditions referring to the operations for purification (Table 1). The procedure was

carried out in accordance with the manual of the senescence β-galactosidase staining kit (Beyotime). This kit allows for the assessment of the degree of cell ageing, as it measures the up-regulated activity level of senescence-associated β-galactosidase, a known marker of cellular senescence.<sup>35</sup>

### **Statistical analysis**

At least three sets of independent experiments were performed for each assay. All quantitative data were analysed by using GraphPad Prism (version 8.0.2 for Windows, GraphPad Software, Boston, MA, USA, www.graphpad.com). Significance of difference between groups was calculated by Student's *t*-test or two-way analysis of variance followed by Bonferroni's multiple comparison test.

## **Results**

### **Morphology of osteo-organoid-derived mesenchymal stem cells**

Cells isolated from osteo-organoids were cultured under hypoxic conditions (5% O<sub>2</sub> and 5% CO<sub>2</sub>), and were purified either by medium refreshment or cell passage (Figure 2A). Specifically, spindle-shaped cells were observed among non-adherent cells before the first medium refresh. Adherent spindle-shaped cells were retained, while most non-adherent cells were washed away. These adherent, spindle-shaped cells were identified as MSCs.<sup>4, 20</sup> When cell confluence reached 70–90%, the cells were observed to be predominantly spindle-shaped, because MSCs proliferate more rapidly than other cells.

### **Proliferation of osteo-organoid-derived mesenchymal stem cells**

The CFU-F assay was utilised to investigate the proportion of MSCs in cells isolated from osteo-organoids, and compared with that from native bone marrow.<sup>20</sup> After a 5-day culture period under normal conditions (21% O<sub>2</sub> and 5% CO<sub>2</sub>), cells stained with toluidine blue were observed under an optical microscope. The control groups, i.e., cells isolated from native bone (Figure 2B), showed a few colonies with a spindle shape, small size and low cell density. In contrast, cells isolated from osteo-organoids formed a significantly larger number of colonies (Figure 2B), which exhibited a slender spindle shape, large scale and high cell density. This phenomenon also suggested that odMSCs had rapid proliferation rates or high abundance at P0.

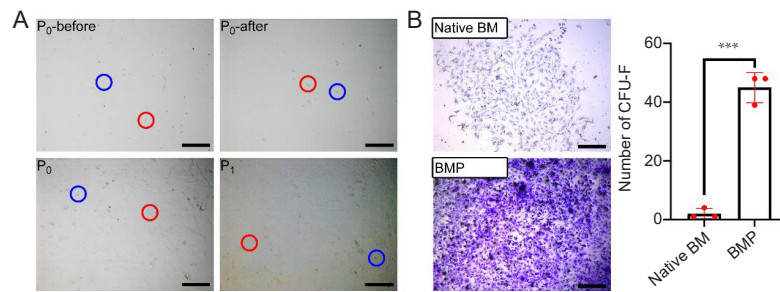


**Figure 2.** Morphology of MSCs and CFU-F assay. (A) Primary cells before (P0-before) and after (P0-after) the first refreshing of the medium, and MSCs at 80% confluence at P0 and P1. Red and blue circles indicate spindle-shaped and round cells. (B) Left: Primary cells from osteo-organoids (constructed with recombinant human bone morphogenetic protein 2-loaded gelatin sponge scaffolds) formed larger colonies than that from bone marrow (native BM). Scale bars: 200 μm. Right: The number of colonies in each well of a standard 6-well plate. Data are expressed as mean ± SD ( $n = 3$ ). \*\*\* $P < 0.001$  (Student's  $t$ -test). CFU-F: colony forming unit-fibroblast; MSCs: mesenchymal stem cells; P: passage.

**Cell surface phenotype and multilineage differentiation of osteo-organoid-derived mesenchymal stem cells**

When 80% confluence at P2, the MSCs cultured in plates were digested and then analysed by flow cytometry. Results showed that the cells from both BM-MSC and odMSC were largely negative for haematopoietic marker CD45, endothelial cell marker CD31, and myeloid cell marker CD11b (Figure 3A). In contrast, the MSC markers (stem cell antigen-1, CD29, CD105, CD44 and CD140a) were strongly positive, and especially the positive rates of stem cell antigen-1 and CD140a of odMSCs were more obvious than those from native BM (Figure 3A). The above result displayed that the cells isolated from osteo-organoids were determinately identified as MSCs, suggesting the successful acquisition of a new stem cell subtype.

To assess the multipotency of the MSCs at P2 (Figure 3B), cells that had reached the appropriate confluence were cultured in various types of differentiation induction media. Alizarin red staining (Figure 3B) and oil red O staining (Figure 3B) demonstrated the primary cells from osteo-organoids (constructed with recombinant human bone morphogenetic protein 2-loaded gelatin sponge scaffolds) showed distinctly more calcified nodules and mature adipocytes than cells from bone marrow did, suggesting that odMSCs had greater osteogenic and adipogenic differentiation capabilities than BM-MSCs did. Concurrently, alcian blue staining of the cartilage revealed that MSCs from both sources had similar chondrogenic differentiation capabilities.

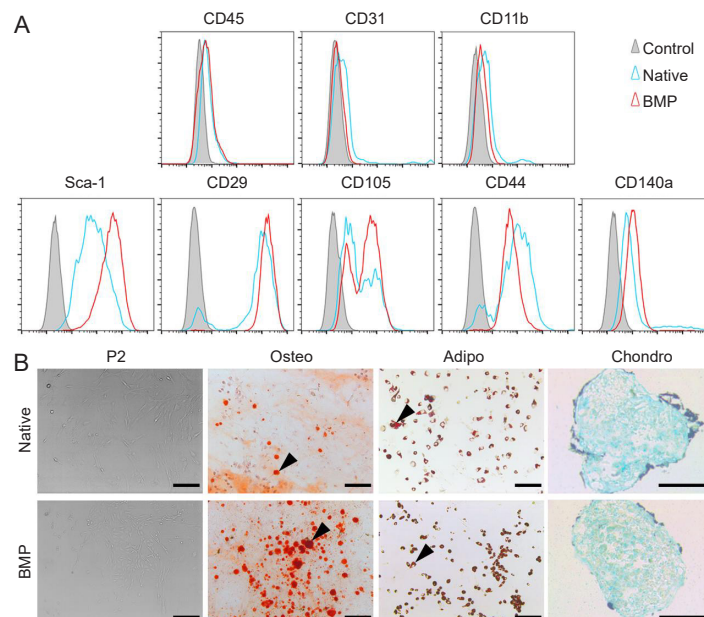


**Figure 3.** Cell surface phenotype and multilineage differentiation of MSCs at P2. (A) Flow cytometry of odMSCs (constructed with recombinant human bone morphogenetic protein 2-loaded gelatin sponge scaffolds; BMP) and bone marrow (native). (B) Alizarin red, oil red O or Alcian blue staining after differentiation under the osteogenic, adipogenic or chondrogenic induction. The osteogenic and adipogenic differentiation of odMSCs were more obvious than that of BM-MSCs. Black triangles indicate calcified nodules and mature adipocytes. Scale bars: 200 μm. BM-MSCs: bone marrow-derived mesenchymal stem cells; MSCs: mesenchymal stem cells; odMSCs: osteo-organoid-derived mesenchymal stem cells; P2: passage 2; Sca-1: stem cell antigen-1.

### Ageing process of osteo-organoid-derived mesenchymal stem cells

In order to assess the ageing process of odMSCs during *in vitro* passage, a senescence-associated  $\beta$ -galactosidase assay was used to evaluate the senescence level of cells from P0 to P2 (Figure 4). From the staining images, it was obvious that native BM-MSCs (native group) had few senescence-associated  $\beta$ -galactosidase positive cells at P0. However, as the passage times increased, the cells gradually aged, and thus showed

noticeable senescence-associated  $\beta$ -galactosidase expression. In contrast, for the odMSCs, light-colored products of  $\beta$ -galactosidase were observed at the P0. Despite this, the ratio of cells expressing  $\beta$ -galactosidase and the depth of blue in odMSCs did not change significantly throughout the passages. From these observations, it can be concluded that unlike BM-MSCs, odMSCs did not exhibit significant ageing during the passage from P0 to P2.

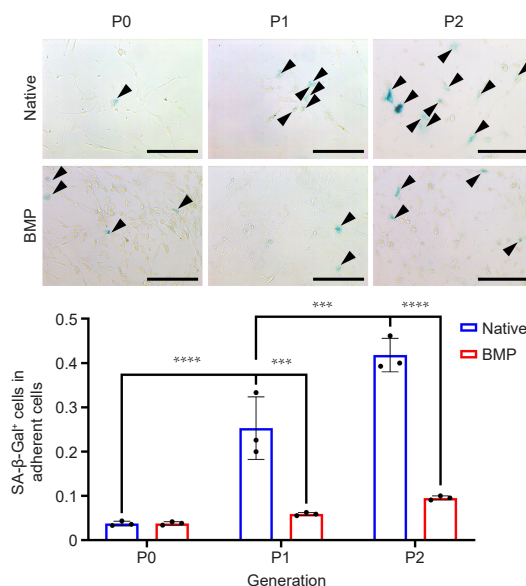


**Figure 4.** Upper: Ageing process for MSCs from P0 to P2. Black triangles indicate SA- $\beta$ -Gal positive cells. Scale bars: 200  $\mu$ m. Lower: The proportions of SA- $\beta$ -Gal positive cells. The proportion of cell senescence in the native BM-MSCs group (native) increased with passage, while it remained basically unchanged in the odMSCs (constructed with recombinant human bone morphogenetic protein 2-loaded gelatin sponge scaffolds; BMP). Data are expressed as mean  $\pm$  SD ( $n = 3$ ). \*\*\*\* $P < 0.0001$ , \*\*\* $P < 0.001$  (two-way analysis of variance followed by Bonferroni's multiple comparison test). BM-MSCs: bone marrow-derived mesenchymal stem cells; odMSCs: osteo-organoid-derived mesenchymal stem cells; P: passage; SA- $\beta$ -Gal: senescence-associated  $\beta$ -galactosidase.

### Cell growth of osteo-organoid-derived mesenchymal stem cells

The odMSCs reached 80% confluence in a shorter time than the BM-MSCs when cultured under hypoxic conditions (Table 3). However, the difference at P0 was greater than at P1. In order to define whether the cell proliferation of odMSCs was still faster than that of BM-MSC after passage, MSCs from both sources at P2 were seeded in 60-mm dish in equal numbers. The MSCs were used for an EdU assay when cell confluence reached 80%, but no more than 100%. The flow

cytometric scatter plots for both groups exhibited a similar horseshoe shape (Figure 5A). Statistical analysis indicated the no significant difference between the proportions of EdU<sup>+</sup> cells in both groups (Figure 5B). The proportion of EdU<sup>+</sup> cells for the BMP group was higher than that of the native group. This was further confirmed by fluorescence images (Figure 5C and D). That is, the total number of cells in odMSCs was higher than that in BM-MSCs, but the proportion of EdU<sup>+</sup> cells in the former was not significantly higher than that in the latter.

**Table 3. Time of mesenchymal stem cell passage from the osteo-organoid vs. native bone marrow**

Source	P0	P1	Total
Osteo-organoid	3 days	3 days	6 days
Native bone marrow	8 days	4 days	12 days

Note: P0: mesenchymal stem cells isolated from an osteo-organoid, or a tibia and a femur; P1: mesenchymal stem cells passaged at a split ratio of 1:3 from P0.

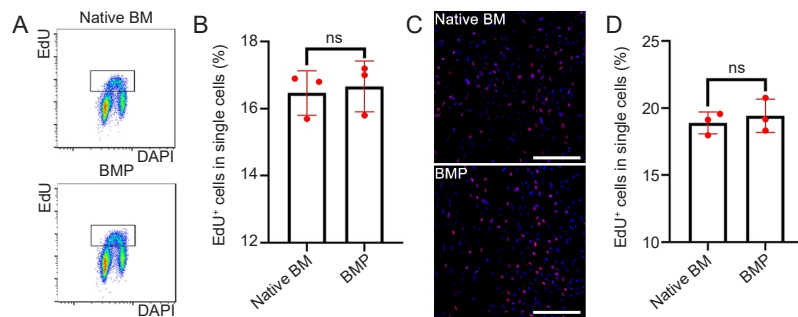


**Figure 5.** Cell proliferation of MSCs at P2. (A, B) Scatter diagrams (A) and content of EdU<sup>+</sup> cells (B) by flow cytometric analysis. (C, D) Fluorescence confocal image (blue: DAPI; red: EdU; C) and statistical analysis (D). Scale bars: 200  $\mu$ m. Data are expressed as mean  $\pm$  SD ( $n = 3$ ), and were analyzed by Student's *t*-test. BM: native bone marrow-derived mesenchymal stem cells; BMP: osteo-organoid-derived mesenchymal stem cells (constructed with recombinant human bone morphogenetic protein 2-loaded gelatin sponge scaffolds); DAPI: 4',6-diamidino-2-phenylindole; EdU: 5-ethynyl-2'-deoxyuridine; MSCs: mesenchymal stem cells; ns: not significant; P2: passage 2.

The above results illustrated that the primary cells played a more important role in proliferation than the cells passed for generations did. In other words, as the native BM group becomes purified, the macroscopic proliferation duration of these MSCs tends to align with that of odMSCs. Last but not least, based on the above results, we could infer that the growth rate of BM-MSCs at P0 was not lower than that of odMSCs, because the former aged faster<sup>36</sup> (Figure 4), while both cell types proliferated at the same rate at P2 (Figure 5). Furthermore, it could be considered that the abundance of odMSCs at P0 was significantly higher than that of BM-MSCs (Figure 2B).

## Discussion

The above results indicate that the MSCs obtained using this method exhibit superior differentiation (Figure 3B) and sufficient proliferation (Figure 5) levels compared with those obtained using traditional methods. Moreover, the osteo-organoid assay yields a higher quantity of MSCs compared with BM-MSCs, since the proportion of primary MSCs to total cells greatly surpasses that of native bone marrow isolated in the same manner (Figure 2B). The number of cells isolated from a tibia and a femur is generally three to four times higher than the cells from osteo-organoids, whereas the latter achieves the same number of MSCs in only half the total time of the former (Table 3). At P2, the proliferation of MSCs from both sources is essentially the same. It was likely because the purity of MSCs with high proliferative activity increases following passage, leading to consistent cell growth rates. BM-MSCs often experience replicative senescence during expansion,<sup>37</sup> which results in a decline in stemness (mainly including capabilities of differentiation, regeneration, proliferation and migration).<sup>38</sup> In contrast, the method described in this paper can reduce the time of *in vitro* expansion to delay the ageing process (Figure 4). The low level of senescence is one reason for the strong differentiation capability of odMSCs at P2. Based on our previous researches, we found that osteo-organoids, after about 1 week of development, exhibit a youthful state and tissue repair activity.<sup>30-32</sup> BM-MSCs are located in the more developed native bone marrow, hence the younger odMSCs

have a high abundance and the ability of anti-replicative senescence.

Compared with the traditional medium, the complete medium used in this protocol was added with Rho-associated kinase inhibitor, as a differentiation inhibitor, and sodium pyruvate and a higher proportion (20%) of fetal bovine serum were used to promote cell growth. The aim is to prevent the loss of stemness due to premature differentiation when MSCs are cultured *in vitro*. Besides, The method eventually purifies stem cells isolated from osteo-organoids, which exhibit a phenotype akin to BM-MSCs (Figure 3A), leading us to classify them as MSCs. However, MSCs from these two sources exhibit some differences in morphology, and the expression levels of cell markers<sup>21, 39</sup> are not entirely consistent. Notably, CD140a, also known as platelet-derived growth factor alpha, is an important marker of myofibroblasts<sup>10, 21, 39, 40</sup> and is highly expressed in odMSCs. The thinner and longer cell morphology of these cells is similar to the classic shape of C2C12 myoblasts cells cultured *in vitro*, which can also respond to bone morphogenetic protein-2 in osteogenesis-related biochemical processes.<sup>34, 40</sup> Therefore, we infer that odMSCs are essentially myogenic MSCs, and they differ from BM-MSCs in terms of cytokine secretion, immunological performance<sup>10, 40</sup> and tissue repair activity.<sup>39, 41</sup> Moreover, the form, structure, composition, and properties of the selected materials are highly customizable, and the implantation time<sup>32</sup> can be selected. In theory, stem cells from different sources or ageing systems can be obtained. For example, we used a gelatin sponge added with chondroitin sulfate and then loaded with rhBMP-2 as a material, and implanted it on the back to create a periosteum-like tissue,<sup>30</sup> enhanced the regenerative capacity of the MSCs. Another example is that we used sulfonated gelatin hydrogel<sup>42</sup> instead of the gelatin sponge to build growth factor-enriched niche, which accelerated bone regeneration. Hence osteo-organoids can be considered an efficient and highly flexible model for studying stem cells such as MSCs.

In the current clinical autologous transplantation methods,<sup>26, 27</sup> the quantity of extracted bone marrow is limited, but patients who need to use MSCs for treatment often have stem cells

## Rapid obtaining strategy of massive MSCs

with insufficient activity. Due to these limitations, MSCs from autologous bone marrow are usually not recommended for stem cell therapy. Even so, compared with allogeneic tissue, autologous tissue is more acceptable to patients due to factors such as higher safety, a simpler application process, better autonomy, and less psychological burden. Although transplantation matching is not required for MSCs usage, non-cryopreserved allogeneic stem cells used for treatments carry some risk from donors.<sup>43</sup> Fresh cells have a limited usage window, thus the transportation efficiency directly impacts the success rate of the operation; the viability and activity of MSCs decrease under cryopreservation conditions,<sup>44</sup> and cell cryopreservation reagents can cause some adverse reactions *in vivo*.<sup>45</sup> Additionally, umbilical cord or adipose-tissue derived MSCs, which are commonly used in stem cell banks, do not exhibit high anti-inflammatory properties as well as BM-MSCs, especially in hypoxic environments.<sup>46</sup> Contrarily, the stem cells obtained through this novel protocol consider the benefits of autologous sources and provide high stem cell quantity and quality, which can be a competitive method for stem cell therapy.

There were still limitations in our study. The odMSCs may come from mixed sources. It is not completely clear the subtype composition and specific of odMSCs. In theory, BM-MSCs should be the main type of odMSCs given that osteo-organoids ultimately form complete bone structures.<sup>47</sup> But in fact, our research has found that odMSCs are likely to be myogenic MSCs. Despite this, the proportion of various MSCs has not been well distinguished. For application, it takes 5 days for osteo-organoids to develop, and not everyone is willing to undergo two surgeries in such a short period of time. Therefore, relevant minimally invasive surgical techniques urgently need to be developed in order to broaden the acceptance of clinical applications.

In conclusion, we constructed osteo-organoids that can generate MSCs in large quantities, high purity, and high quality by means of *in vivo* tissue engineering. The odMSCs can be used in the *in vitro* study of stem cells through simple purification, and odMSCs maintain youthful states during short-term *in vitro* expansion, which will contribute to research and applications on reversing senescence. On this basis, more researches, such as the myoideum source characterisation, bone marrow ablation models, and scaffold materials modification, are underway. Furthermore, for clinical application, this method is a fast way to harvest high density of stem cells. Therefore, this study provides an alternative protocol for obtaining large quantities of and high quality MSCs and is expected to be a novel solution for stem cell therapy.

**Author contributions**

SD: investigation, experiments, analysis, validation, writing and editing; FZ: experiments; KD: investigation, experiments, validation and writing; JW: funding acquisition, resources, supervision, review, and editing; CL: funding acquisition, resources, supervision, review, and editing. All authors discussed the results, commented on the manuscript, and approved the final version of the manuscript.

**Financial support**

This study was supported by the Basic Science Center Program of National Natural Science Foundation of China, No. T2288102, the Key Program of the National Natural Science Foundation of China, No. 32230059, the Foundation

of Frontiers Science Center for Materiobiology and Dynamic Chemistry, No. JKVD1211002, the Wego Project of Chinese Academy of Sciences, No. (2020) 005, the National Natural Science Foundation of China, No. 32301123, the China Postdoctoral Science Foundation, No. 2022M721147, and the Project of National Facility for Translational Medicine (Shanghai), No. TMSK-2021-134.

**Acknowledgement**

We thank Professor Rui Yue's research group at Tongji University for their careful guidance of isolation cells from bone marrow and epiphysis using digestive enzyme mixture.

**Conflicts of interest statement**

There are no conflicts to declare.

**Editor note:** Changsheng Liu is an Editorial Board member of *Biomaterials Translational*. He was blinded from reviewing or making decisions on the manuscript. The article was subject to the journal's standard procedures, with peer review handled independently of this Editorial Board member and his research group.

**Open access statement**

This is an open access journal, and articles are distributed under the terms of the Creative Commons Attribution-NonCommercial-ShareAlike 4.0 License, which allows others to remix, tweak, and build upon the work non-commercially, as long as appropriate credit is given and the new creations are licensed under the identical terms.

- Zhu, H.; Guo, Z. K.; Jiang, X. X.; Li, H.; Wang, X. Y.; Yao, H. Y.; Zhang, Y.; Mao, N. A protocol for isolation and culture of mesenchymal stem cells from mouse compact bone. *Nat Protoc.* **2010**, *5*, 550-560.
- Li, W. Y.; Choi, Y. J.; Lee, P. H.; Huh, K.; Kang, Y. M.; Kim, H. S.; Ahn, Y. H.; Lee, G.; Bang, O. Y. Mesenchymal stem cells for ischemic stroke: changes in effects after ex vivo culturing. *Cell Transplant.* **2008**, *17*, 1045-1059.
- Kurth, T. B.; Dell'accio, F.; Crouch, V.; Augello, A.; Sharpe, P. T.; De Bari, C. Functional mesenchymal stem cell niches in adult mouse knee joint synovium in vivo. *Arthritis Rheum.* **2011**, *63*, 1289-1300.
- Huang, S.; Xu, L.; Sun, Y.; Wu, T.; Wang, K.; Li, G. An improved protocol for isolation and culture of mesenchymal stem cells from mouse bone marrow. *J Orthop Translat.* **2015**, *3*, 26-33.
- Rossi, C. A.; Flaibani, M.; Blaauw, B.; Pozzobon, M.; Figallo, E.; Reggiani, C.; Vitiello, L.; Elvassore, N.; De Coppi, P. In vivo tissue engineering of functional skeletal muscle by freshly isolated satellite cells embedded in a photopolymerizable hydrogel. *FASEB J.* **2011**, *25*, 2296-2304.
- Zhai, W.; Yong, D.; El-Jawhari, J. J.; Cuthbert, R.; McGonagle, D.; Win Naing, M.; Jones, E. Identification of senescent cells in multipotent mesenchymal stromal cell cultures: current methods and future directions. *Cytotherapy.* **2019**, *21*, 803-819.
- Karnoub, A. E.; Dash, A. B.; Vo, A. P.; Sullivan, A.; Brooks, M. W.; Bell, G. W.; Richardson, A. L.; Polyak, K.; Tubo, R.; Weinberg, R. A. Mesenchymal stem cells within tumour stroma promote breast cancer metastasis. *Nature.* **2007**, *449*, 557-563.
- Salazar-Noratto, G. E.; Luo, G.; Denoed, C.; Padrona, M.; Moya, A.; Bensidhoum, M.; Bizios, R.; Potier, E.; Logeart-Avramoglou, D.; Petite, H. Understanding and leveraging cell metabolism to enhance mesenchymal stem cell transplantation survival in tissue engineering and regenerative medicine applications. *Stem Cells.* **2020**, *38*, 22-33.
- Wang, Y.; Zhang, W.; Yao, Q. Copper-based biomaterials for bone and cartilage tissue engineering. *J Orthop Translat.* **2021**, *29*, 60-71.
- Uezumi, A.; Fukada, S.; Yamamoto, N.; Takeda, S.; Tsuchida, K. Mesenchymal progenitors distinct from satellite cells contribute to ectopic fat cell formation in skeletal muscle. *Nat Cell Biol.* **2010**, *12*, 143-152.

11. Tidu, F.; De Zuani, M.; Jose, S. S.; Bendíčková, K.; Kubala, L.; Caruso, F.; Cavalieri, F.; Forte, G.; Frič, J. NFAT signaling in human mesenchymal stromal cells affects extracellular matrix remodeling and antifungal immune responses. *iScience*. **2021**, *24*, 102683.
12. Wang, G.; Cao, K.; Liu, K.; Xue, Y.; Roberts, A. I.; Li, F.; Han, Y.; Rabson, A. B.; Wang, Y.; Shi, Y. Kynurenic acid, an IDO metabolite, controls TSG-6-mediated immunosuppression of human mesenchymal stem cells. *Cell Death Differ*. **2018**, *25*, 1209-1223.
13. Kfoury, Y.; Scadden, D. T. Mesenchymal cell contributions to the stem cell niche. *Cell Stem Cell*. **2015**, *16*, 239-253.
14. McCullen, S. D.; Chow, A. G.; Stevens, M. M. In vivo tissue engineering of musculoskeletal tissues. *Curr Opin Biotechnol*. **2011**, *22*, 715-720.
15. Li, Z.; Niu, S.; Guo, B.; Gao, T.; Wang, L.; Wang, Y.; Wang, L.; Tan, Y.; Wu, J.; Hao, J. Stem cell therapy for COVID-19, ARDS and pulmonary fibrosis. *Cell Prolif*. **2020**, *53*, e12939.
16. Hejcl, A.; Sedý, J.; Kapcalová, M.; Toro, D. A.; Amemori, T.; Lesný, P.; Likavcanová-Mašínová, K.; Krumbholcová, E.; Prádný, M.; Michálek, J.; Burian, M.; Hájek, M.; Jendelová, P.; Syková, E. HPMA-RGD hydrogels seeded with mesenchymal stem cells improve functional outcome in chronic spinal cord injury. *Stem Cells Dev*. **2010**, *19*, 1535-1546.
17. Maruyama, M.; Pan, C. C.; Moeinzadeh, S.; Storaci, H. W.; Guzman, R. A.; Lui, E.; Ueno, M.; Utsunomiya, T.; Zhang, N.; Rhee, C.; Yao, Z.; Takagi, M.; Goodman, S. B.; Yang, Y. P. Effect of porosity of a functionally-graded scaffold for the treatment of corticosteroid-associated osteonecrosis of the femoral head in rabbits. *J Orthop Translat*. **2021**, *28*, 90-99.
18. Sun, L.; Akiyama, K.; Zhang, H.; Yamaza, T.; Hou, Y.; Zhao, S.; Xu, T.; Le, A.; Shi, S. Mesenchymal stem cell transplantation reverses multiorgan dysfunction in systemic lupus erythematosus mice and humans. *Stem Cells*. **2009**, *27*, 1421-1432.
19. Cao, X.; Duan, L.; Hou, H.; Liu, Y.; Chen, S.; Zhang, S.; Liu, Y.; Wang, C.; Qi, X.; Liu, N.; Han, Z.; Zhang, D.; Han, Z. C.; Guo, Z.; Zhao, Q.; Li, Z. IGF-1C hydrogel improves the therapeutic effects of MSCs on colitis in mice through PGE(2)-mediated M2 macrophage polarization. *Theranostics*. **2020**, *10*, 7697-7709.
20. Soleimani, M.; Nadri, S. A protocol for isolation and culture of mesenchymal stem cells from mouse bone marrow. *Nat Protoc*. **2009**, *4*, 102-106.
21. Houlihan, D. D.; Mabuchi, Y.; Morikawa, S.; Niibe, K.; Araki, D.; Suzuki, S.; Okano, H.; Matsuzaki, Y. Isolation of mouse mesenchymal stem cells on the basis of expression of Sca-1 and PDGFR- $\alpha$ . *Nat Protoc*. **2012**, *7*, 2103-2111.
22. Lin, W.; Xu, L.; Lin, S.; Shi, L.; Wang, B.; Pan, Q.; Lee, W. Y. W.; Li, G. Characterisation of multipotent stem cells from human peripheral blood using an improved protocol. *J Orthop Translat*. **2019**, *19*, 18-28.
23. Matsuda, K.; Falkenberg, K. J.; Woods, A. A.; Choi, Y. S.; Morrison, W. A.; Dilley, R. J. Adipose-derived stem cells promote angiogenesis and tissue formation for in vivo tissue engineering. *Tissue Eng Part A*. **2013**, *19*, 1327-1335.
24. Lin, W.; Xu, L.; Li, G. A novel protocol for isolation and culture of multipotent progenitor cells from human urine. *J Orthop Translat*. **2019**, *19*, 12-17.
25. Xu, Y.; Zhang, T.; Chen, Y.; Shi, Q.; Li, M.; Qin, T.; Hu, J.; Lu, H.; Liu, J.; Chen, C. Isolation and characterization of multipotent canine urine-derived stem cells. *Stem Cells Int*. **2020**, *2020*, 8894449.
26. Huang, R. L.; Kobayashi, E.; Liu, K.; Li, Q. Bone graft prefabrication following the in vivo bioreactor principle. *EBioMedicine*. **2016**, *12*, 43-54.
27. Yin, J. Q.; Zhu, J.; Ankrum, J. A. Manufacturing of primed mesenchymal stromal cells for therapy. *Nat Biomed Eng*. **2019**, *3*, 90-104.
28. Mauney, J. R.; Nguyen, T.; Gillen, K.; Kirker-Head, C.; Gimple, J. M.; Kaplan, D. L. Engineering adipose-like tissue in vitro and in vivo utilizing human bone marrow and adipose-derived mesenchymal stem cells with silk fibroin 3D scaffolds. *Biomaterials*. **2007**, *28*, 5280-5290.
29. Cui, L.; Xiang, S.; Chen, D.; Fu, R.; Zhang, X.; Chen, J.; Wang, X. A novel tissue-engineered bone graft composed of silicon-substituted calcium phosphate, autogenous fine particulate bone powder and BMSCs promotes posterolateral spinal fusion in rabbits. *J Orthop Translat*. **2021**, *26*, 151-161.
30. Dai, K.; Deng, S.; Yu, Y.; Zhu, F.; Wang, J.; Liu, C. Construction of developmentally inspired periosteum-like tissue for bone regeneration. *Bone Res*. **2022**, *10*, 1.
31. Dai, K.; Shen, T.; Yu, Y.; Deng, S.; Mao, L.; Wang, J.; Liu, C. Generation of rhBMP-2-induced juvenile ossicles in aged mice. *Biomaterials*. **2020**, *258*, 120284.
32. Dai, K.; Zhang, Q.; Deng, S.; Yu, Y.; Zhu, F.; Zhang, S.; Pan, Y.; Long, D.; Wang, J.; Liu, C. A BMP-2-triggered in vivo osteo-organoid for cell therapy. *Sci Adv*. **2023**, *9*, eadd1541.
33. Dey, D.; Bagarova, J.; Hatsell, S. J.; Armstrong, K. A.; Huang, L.; Ermann, J.; Vonner, A. J.; Shen, Y.; Mohedas, A. H.; Lee, A.; Eekhoff, E. M.; van Schie, A.; Demay, M. B.; Keller, C.; Wagers, A. J.; Economides, A. N.; Yu, P. B. Two tissue-resident progenitor lineages drive distinct phenotypes of heterotopic ossification. *Sci Transl Med*. **2016**, *8*, 366ra163.
34. Smith, E.; Yang, J.; McGann, L.; Sebal, W.; Uludag, H. RGD-grafted thermoreversible polymers to facilitate attachment of BMP-2 responsive C2C12 cells. *Biomaterials*. **2005**, *26*, 7329-7338.
35. Zhou, B. O.; Yue, R.; Murphy, M. M.; Peyer, J. G.; Morrison, S. J. Leptin-receptor-expressing mesenchymal stromal cells represent the main source of bone formed by adult bone marrow. *Cell Stem Cell*. **2014**, *15*, 154-168.
36. Leong, D. J.; Sun, H. B. Mesenchymal stem cells in tendon repair and regeneration: basic understanding and translational challenges. *Ann N Y Acad Sci*. **2016**, *1383*, 88-96.
37. Wagner, W.; Horn, P.; Castoldi, M.; Diehlmann, A.; Bork, S.; Saffrich, R.; Benes, V.; Blake, J.; Pfister, S.; Eckstein, V.; Ho, A. D. Replicative senescence of mesenchymal stem cells: a continuous and organized process. *PLoS One*. **2008**, *3*, e2213.
38. Dimri, G. P.; Lee, X.; Basile, G.; Acosta, M.; Scott, G.; Roskelley, C.; Medrano, E. E.; Linskens, M.; Rubelj, I.; Pereira-Smith, O.; et al. A biomarker that identifies senescent human cells in culture and in aging skin in vivo. *Proc Natl Acad Sci U S A*. **1995**, *92*, 9363-9367.
39. Julien, A.; Kanagalingam, A.; Martínez-Sarrà, E.; Megret, J.; Luka, M.; Ménager, M.; Relaix, F.; Colnot, C. Direct contribution of skeletal muscle mesenchymal progenitors to bone repair. *Nat Commun*. **2021**, *12*, 2860.
40. Wang, X.; Matthews, B. G.; Yu, J.; Novak, S.; Grcevic, D.; Sanjay, A.; Kalajzic, I. PDGF modulates BMP2-induced osteogenesis in periosteal progenitor cells. *JBMR Plus*. **2019**, *3*, e10127.
41. Lees-Shepard, J. B.; Yamamoto, M.; Biswas, A. A.; Stoessel, S. J.; Nicholas, S. E.; Cogswell, C. A.; Devarakonda, P. M.; Schneider, M. J., Jr.; Cummins, S. M.; Legendre, N. P.; Yamamoto, S.; Kaartinen, V.; Hunter, J. W.; Goldhamer, D. J. Activin-dependent signaling in fibro/adipogenic progenitors causes fibrodysplasia ossificans progressiva. *Nat Commun*. **2018**, *9*, 471.
42. Zhang, Q.; Liu, Y.; Li, J.; Wang, J.; Liu, C. Recapitulation of growth

## Rapid obtaining strategy of massive MSCs

- factor-enriched microenvironment via BMP receptor activating hydrogel. *Bioact Mater.* **2023**, *20*, 638-650.
43. Fernández-Santos, M. E.; García-Arranz, M.; Andreu, E. J.; García-Hernández, A. M.; López-Parra, M.; Villarón, E.; Sepúlveda, P.; Fernández-Avilés, F.; García-Olmo, D.; Prosper, F.; Sánchez-Guijo, F.; Moraleda, J. M.; Zapata, A. G. Optimization of mesenchymal stromal cell (MSC) manufacturing processes for a better therapeutic outcome. *Front Immunol.* **2022**, *13*, 918565.
  44. Saha, D.; Hofmann, N.; Mueller, T.; Niemann, H.; Glasmacher, B. C-2014: Investigation of genetic and epigenetic changes of cryopreserved mesenchymal stem cells. *Cryobiology.* **2014**, *69*, 519.
  45. Shu, Z.; Heimfeld, S.; Gao, D. Hematopoietic SCT with cryopreserved grafts: adverse reactions after transplantation and cryoprotectant removal before infusion. *Bone Marrow Transplant.* **2014**, *49*, 469-476.
  46. Lagonda, C. A.; Tjahjadi, F. B.; Fauza, D.; Kusnadi, Y. Hypoxia increases vegf secretion in multiple sources of mesenchymal stem cell. *Cytotherapy.* **2018**, *20*, S44-S45.
  47. Wang, X.; Li, F.; Xie, L.; Crane, J.; Zhen, G.; Mishina, Y.; Deng, R.; Gao, B.; Chen, H.; Liu, S.; Yang, P.; Gao, M.; Tu, M.; Wang, Y.; Wan, M.; Fan, C.; Cao, X. Inhibition of overactive TGF- $\beta$  attenuates progression of heterotopic ossification in mice. *Nat Commun.* **2018**, *9*, 551.

Received: September 21, 2023

Revised: November 14, 2023

Accepted: November 30, 2023

Available online: December 28, 2023